Improving Occupancy Grid Mapping via dynamical dithering

Stefano Sabatini, Matteo Corno and Sergio Matteo Savaresi[1]

***Abstract*— Occupancy grid maps are by far the most used spatial representation of the environment for robot navigation. This paper proposes a simple and effective way to improve the occupancy grid accuracy by superimposing a small oscillation to the robot motion when a predefined path is given. The method is especially suited for range sensors with long range capabilities but poor angular resolution. The innovative solid state LiDAR technology is an example of such sensor configuration and is used in this work for the experimental evaluation of the presented dithering technique. Experimental results quantitatively demonstrated that the proposed oscillating motion is effective especially in speeding up the detection of corridor like clearances in the environment.**

I. INTRODUCTION

A key aspect in autonomous robot navigation is the spatial representation of the environment. The ability of the robot to safely navigate in it is strongly related to the accuracy of the map available to the path planner. In order to create a good map, a reliable estimation of the robot location is required: uncertainties therefore reside not only in the sensing capabilities of the surrounding environment but also in the knowledge of the instantaneous robot pose. Consequently, the estimation of the map and of the robot pose is usually performed jointly in the so-called SLAM process (Simultaneous Localization And Mapping). Many SLAM algorithms make use of occupancy grid maps as spatial representation (e.g. [1] and [2]). Occupancy grid maps are one of the most popular spatial representation used in the robotics community because they are able to account for sensing uncertainties in a simple and effective manner. The idea is to represent the environment as an evenly spaced field of binary random variables (called cells) indicating the presence of an obstacle at that location. This mapping technique was first developed by Elfes in [3] as a tentative to cope with incorrect and noisy measurements returned by sonar sensors. One of the most challenging problem in occupancy grid mapping is dealing with the uncertainties that originates from sensors with poor angular resolution. Another important aspect of SLAM algorithms is that the robot trajectory during the mapping process is usually given a priori: the robot is either manually operated or driven by an exploration heuristics (e.g. frontier based exploration algorithms).

The objective of this paper is to experimentally evaluate the advantages of superimposing a small oscillating high frequency path to an a priori selected path in order to improve the accuracy of the occupancy grid map. This approach turns out to be useful especially when the range sensors utilized are characterized by low angular resolution. These sensors return a detection distance corresponding to an object that can be anywhere inside a fairly wide detection cone (it can be up to 25 ° for some sonar sensors): in this case small clearance like corridors may not be visible especially from long distances as highlighted in Figure 1. The idea is that a small dither in the trajectory can help in periodically aligning the detection cone axis with the clearance, maximizing its probability of detection.

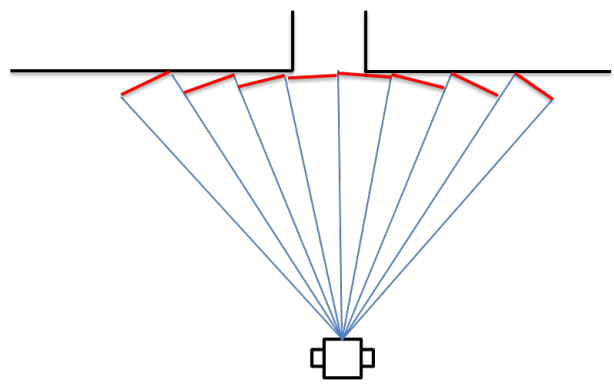

Fig. 1. Situation where a low angular resolution sensor cannot detect a clearance like a corridor in the environment.

The mentioned dithering techinique can be useful not only during a mapping process of an area but also in case of a local obstacle avoidance algorithm that may rely on a local map generated from range sensors (see for example the popular Vector Field Histogram approach described in [8]). In such algorithms detecting or not a clearance may substantially vary the chosen path. To give a complete overview of the mapping problem, there are also some more general and formal methods to select an adequate trajectory for exploration that can be grouped under the name of active SLAM (see [9], [10]): these algorithms tries to solve an optimization problem in order to find the best autonomous path that minimize the resulting map uncertainty (often estimated through the Shannon entropy [11]). These kind of approaches can be very complex since they involve an optimization in an high dimensional space while the dithering approach described here is intended to be a simple way to improve the detection of clearances when an exploration path is already given. In the paper the pose of the robot is considered perfectly known but the idea can be easily extended to solve the full SLAM problem.

Another originality consists in the sensor setup: the experimental data presented in this work are collected with the

[1]Dipartimento Elettronica Informazione e Bioingegneria, Politecnico di Milano , via Ponzio 34/5, 20133, Milano, Italy. stefano.sabatini, matteo.corno, sergio.savaresi@polimi.it

LiDAR LeddarVu8 that belongs to the innovative category of solid state laser range finder that are meant to dominate the LiDAR market in the next years. These sensors are characterized by a much longer range and improved reliability compared to sonar sensors but, thanks to the absence of moving parts, they are much cheaper than traditional laser scanners. Up to now only limited angular resolution are present on the market (12.5 ° in the considered set-up) motivating the use of the dithering technique here presented. The paper is structured as follows: Section II reviews the common approach to occupancy grid mapping, in Section III the description and modeling of the solid state LiDAR utilized is presented. Section IV demonstrate qualitatively and quantitatively the mapping results with and without dithering.

II. OCCUPANCY GRID MAPPING

The general occupancy map problem can be casted into the Bayesian inference theory. In this framework, the problem of estimating the map m can be expressed by the following posterior:

$$p(m|x_{1:t}, z_{1:t}) \tag{1}$$

where $x_{1:t}$ and $z_{1:t}$ stands for the robot poses and measurements respectively from the time instant 1 up to t. The original formulation by Elfes in [3], makes the assumption of mutual independence between cells. Thanks to this strong assumption, the mapping problem is reduced from an estimation problem in the high dimensional space of all possible maps to many one-dimensional estimation problem corresponding to the occupancy of the single cell m_{ij}:

$$p(m|x_{1:t}, z_{1:t}) = \prod_{ij} p(m_{ij}|z_{1:t}, x_{1:t}) \tag{2}$$

The probability of occupancy of a single cell can be derived applying Bayesian reasoning, the full derivation is not reported here and it is well explained in [12]. The result is a recursive formula expressed in log-odds ratios l^t_{ij}:

$$l^t_{ij} = log(\frac{p(m_{ij}|x_{1:t}, z_{1:t})}{1 - p(m_{ij}|x_{1:t}, z_{1:t})}) = l^{t-1}_{ij} + log(\frac{p(m_{ij}|z_t, x_t)}{1 - p(m_{ij}|z_t, x_t)}) \tag{3}$$

where in writing (3) the prior knowledge of the map occupancy $p(m_{ij})$ was set to 0.5 indicating an initial unknown state. Equation (3) states that, under the assumption of cell mutual independence and static map, the cell probability can be updated incrementally adding to the current knowledge of the cell occupancy l^{t-1}_{ij}, the information coming from the latest measurement z_t carried by the term $p(m_{ij}|x_t, z_t)$. The quantity $p(m_{ij}|x_t, z_t)$ is usually called *inverse sensor model* because it maps the latest sensor measurement back to its cause specifying the probability of occupancy of the cell ij conditioned to the measured z_t.

Different improvements and extension to this formulation are presented in literature, especially to better deal with the uncertainties coming from sonar measurements due to their poor angular resolution, e.g [4], [5]. A well known approach in this sense, in clear contrast with the presented formulation, is the one presented by Thrun in [6]: here the author makes use of the so-called *forward sensor model* $p(z_t|m)$ and solves the mapping problem directly in the high dimensional space. A comparison of the performance of different grid mapping algorithm is present in [7] where the superior performance of a forward-sensor model approach are demonstrated. Despite its inferior accuracy, the log-odds update rule based on the inverse sensor model is still the most used in practice: its simplicity, low computational burden and recursive formulation allow real-time implementation. Therefore in this work the inverse sensor model formulation described by (3) is used to compute the occupancy grid map update. An approach simlar to what presented in [6] has not been pursued because, due to the lack of in depth technical information about the solid state LiDAR employed, defining the expression of the forward model resulted cumbersome. In absensce of an accurate forward model, the theoretical superiority of the approach may not be reflected in practice.

III. SENSOR SETUP AND INVERSE MODEL

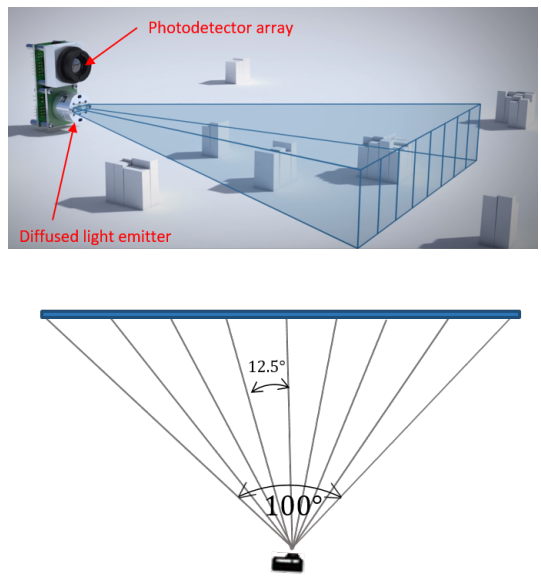

Fig. 2. Schematic of the LeddarVu8 functionig. In the top figure, the sensor is depicted with the main components highlighted. In the bottom figure a top view of the sensor field of view.

The Laser sensor used in this work is the LeddarVu8, a 2D solid state LiDAR by the Canadian company Leddartech [13]. As most of the LiDAR technologies, this sensor works with the time of flight principle. Compared to common mechanical laser scanners the LeddarVu8 does not present any rotating parts but it employs the so-called flash LiDAR technology. This technology consists in using a single fixed beam light source that is diffused through the use of an appropriate optics over a field of view of 100 degrees. The total field of view is divided in 8 detection segments: the sensor is ~~infact~~ provided by an array of eight independent photo-detectors that receive and process the light reflected by objects in the field of view. The detection frequency depends

on some parameters that can be set-up by the user in order to select the most suitable trade-off between sampling rate and accuracy. As a result of our tuning, the sensors returns 8 detection distances at a frequency of 10 Hz with an angular resolution of 12.5 degrees. A scheme depicting the sensor functioning is presented in Figure 2. The specific version of the sensor used is capable of detecting obstacle up to 34 m of distance.

As introduced in the previous section, the inverse sensor model $p(m_{ij}|z_t, x_t)$ describes the probability that a cell is occupied conditioned to the measured z_t. The poor angular resolution of 12.5 °, around 100 times lower than common laser scanners, originates a substantial angular uncertainty: given a measurement, many cells belonging to the same segment may be the cause of that detection, especially at long ranges. This fact motivated the decision of using an inverse sensor model similar to what has been presented for other wide-beam sensors like sonar or radars. The inverse sensor model here employed is the one described in [14]. Each detection segment is treated separately and the update probability $p(m_{ij}|z_t, x_t)$ depends on the position of the cell inside the detection beam described in polar coordinates through the tuple (d, θ) (see Figure 3).

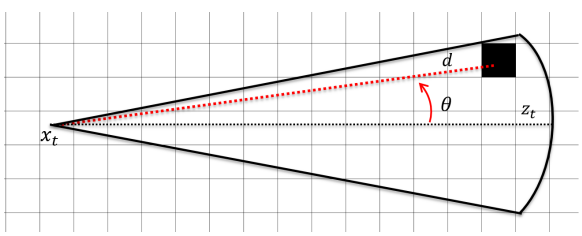

Fig. 3. Detection beam defined by a measurement. The position of a cell inside the beam is defined in polar coordinates.

The sensor model is than defined piece-wise as follows:

$$p(m_{ij}|z_t, x_t) = 0.5 + \begin{cases} -s(z_t, \theta) & d < z_t - d_1 \\ -s(z_t, \theta) + \frac{s(z_t, \theta)}{d_1}(d - z_t + d_1) & d < z_t + d_2 \\ +s(z_t, \theta) & d < z_t - d_1 \\ +s(z_t, \theta) - \frac{s(z_t, \theta)}{d_3 - d_2}(d - z_t + d_2) & d < z_t + d_3 \\ 0 & \text{otherwise} \end{cases} \tag{4}$$

where $s(z_t, \theta)$ depends linearly on the measured range through $g(z_t)$ and on the angular position through a Gaussian distribution centered on the beam axis:

$$s(z_t, \theta) = g(z_t)\mathcal{N}(0, \sigma_\theta) \tag{5}$$

Figure 4 shows the probability update for a single measurement occured at 7 meters: cells closer than the measured distance are assigned a low occupancy probability (smaller than the prior $p(m_{ij}) = 0.5$) and cells around the measured distance are assigned a~~n~~ high occupancy probability. Morover, with the definition of $s(z_t, \theta)$ in Equation (5), shorter measurements provides higher probability updates and cells closer to the beam axis are given a higher probability of occupancy compared to the one on the edges.

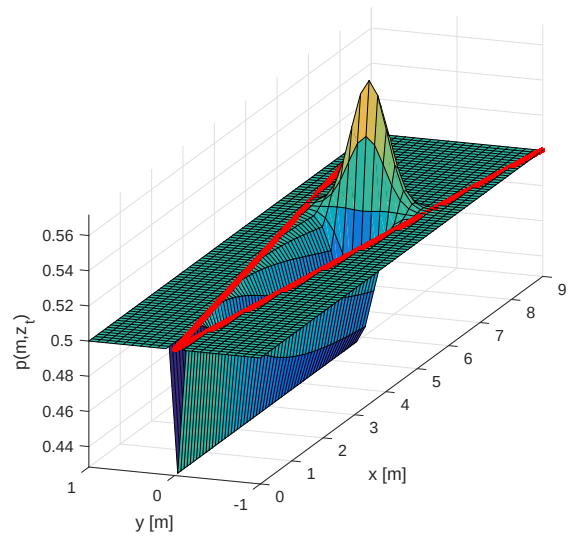

Fig. 4. Representation of an occupancy grid update through the inverse sensor model described in Equation (4) for a measurement occurred at 7 m. Straigth red lines delimit a single detection segment.

IV. EXPERIMETAL EVALUATION OF THE DITHERING MAPPING

This section is dedicated to the description of the experiments performed to evaluate the benefit of the dithering technique. First, the description of how the mechanical dither is applied to the robot is provided. Then, a specific map evaluation metric is defined and finally the mapping performance of the robot with the dithering motion are evaluated in a specific case and compared with a nominal case when the dither is not applied.

A. Applying the dither

Fig. 5. The two wheeled self-balancing robot used in the experiments. The mounting position of the LiDAR is highlighted.

All the experiments were performed using a two wheeled self balancing robot depicted in Figure 5. The two wheel configuration is of great importance in this context because,

thanks to the differential drive capability, the robot is very agile.

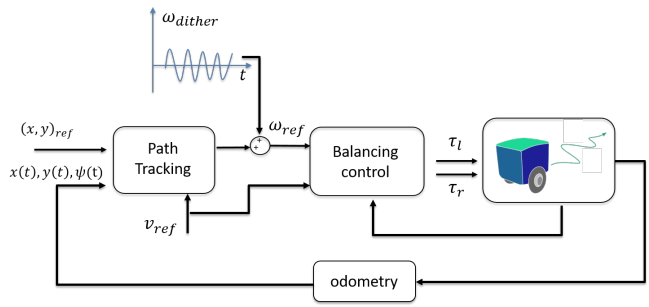

Fig. 6. Robot control scheme for path tracking task. The dithering trajectory is added as an angular speed reference oscillation.

The robot control system has been implemented in a cascade manner as depicted in Figure 6. The outer loop is the path tracking control that, based on the posture estimate, decides the angular velocity reference ω_{ref} in order to follow, at a pre-defined speed, a desired path specified in the Cartesian plane (see [15] for details on the path tracking implementation). The inner control loop consists in the balancing control that has the task of actuating the velocities references through the wheel torques, while keeping the robot in equilibrium. The dithering trajectory is actuated adding an high frequency sinusoidal signal ω_{dither} to the reference angular speed as specified in Figure 6.

Since the frequency of the dither is much higher than the bandwidth of the path tracking loop, a dithering trajectory results superimposed to the reference path. The resulting robot motion is shown in figure 7: while the robot path seems almost perfectly overlapped to the reference, an oscillation corresponding to the applied dither is clearly visible around the robot orientation requested by the reference path.

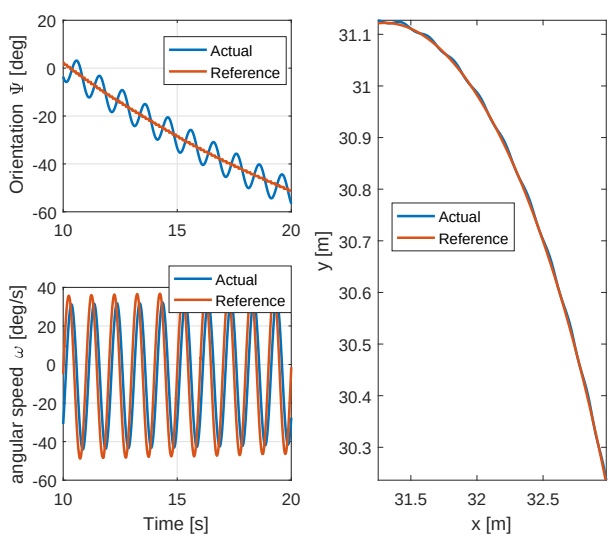

Fig. 7. Resulting robot trajectory when a dither is applied.

B. Map evaluation criteria

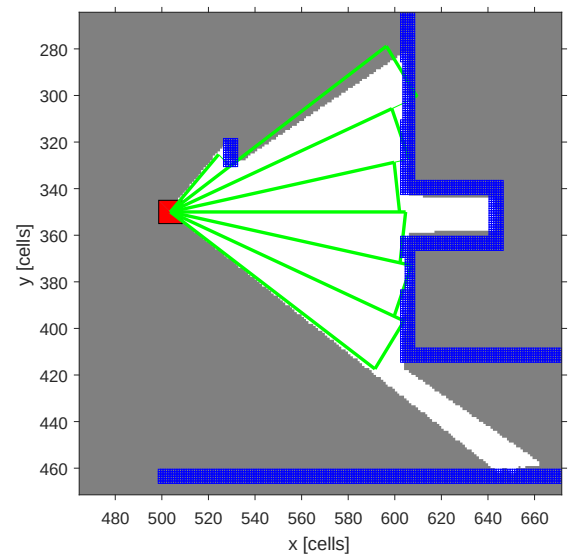

Fig. 8. Definition of spanned region. The red square corresponds to the robot position, the green sectors corresponds to the measurements returned by the LiDAR, the blu cells corresponds to the ground truth walls and the spanned region is highlighted in white.

In this section, a map evaluation metric is defined in order to compare different mapping results and highlights quantitatively the advantages of performing a dithering motion. Defining a map metric is not as trivial as it may seems, different methods described in literature are reviewed in [16]. The method described here is based on a pixel to pixel comparison to a ground truth reconstructed by hand through direct measurements of distances and walls length. The metric takes inspiration from the Overall Error quantity described in [17] where it was defined as the summation over the considered map of the cell to cell error calculated as the difference between the probability of occupancy in the estimated map and the ground truth. As highlighted in [7], this formulation carries an intrinsic problem: in general the amount of empty space in an environment is largely superior to the amount of objects and walls, therefore a merit function that considers in the same way all the cells will somehow underrate the occupied space. This fact leads to the definition of Weighted Overall Error WOE where each cell contribution to the total error is weighted by the occupancy ratio OR calculated based on the ground truth map:

$$WOE = \frac{(1-OR)\sum_{occ}|p(m_{ij}) - m_{ij_{gt}}| + OR\sum_{emp}|p(m_{ij}) - m_{ij_{gt}}|}{\#\text{ of cells}} \tag{6}$$

With this formulation, cells that are estimated as occupied ($p(m_{ij}) > 0.5$) have more weight in the total WOE.

The final objective is to compare mapping results produced with different robot trajectories, in the specific case a non dithering - dithering comparison must be performed. A trajectory with a superimposed dither most probably will scan a

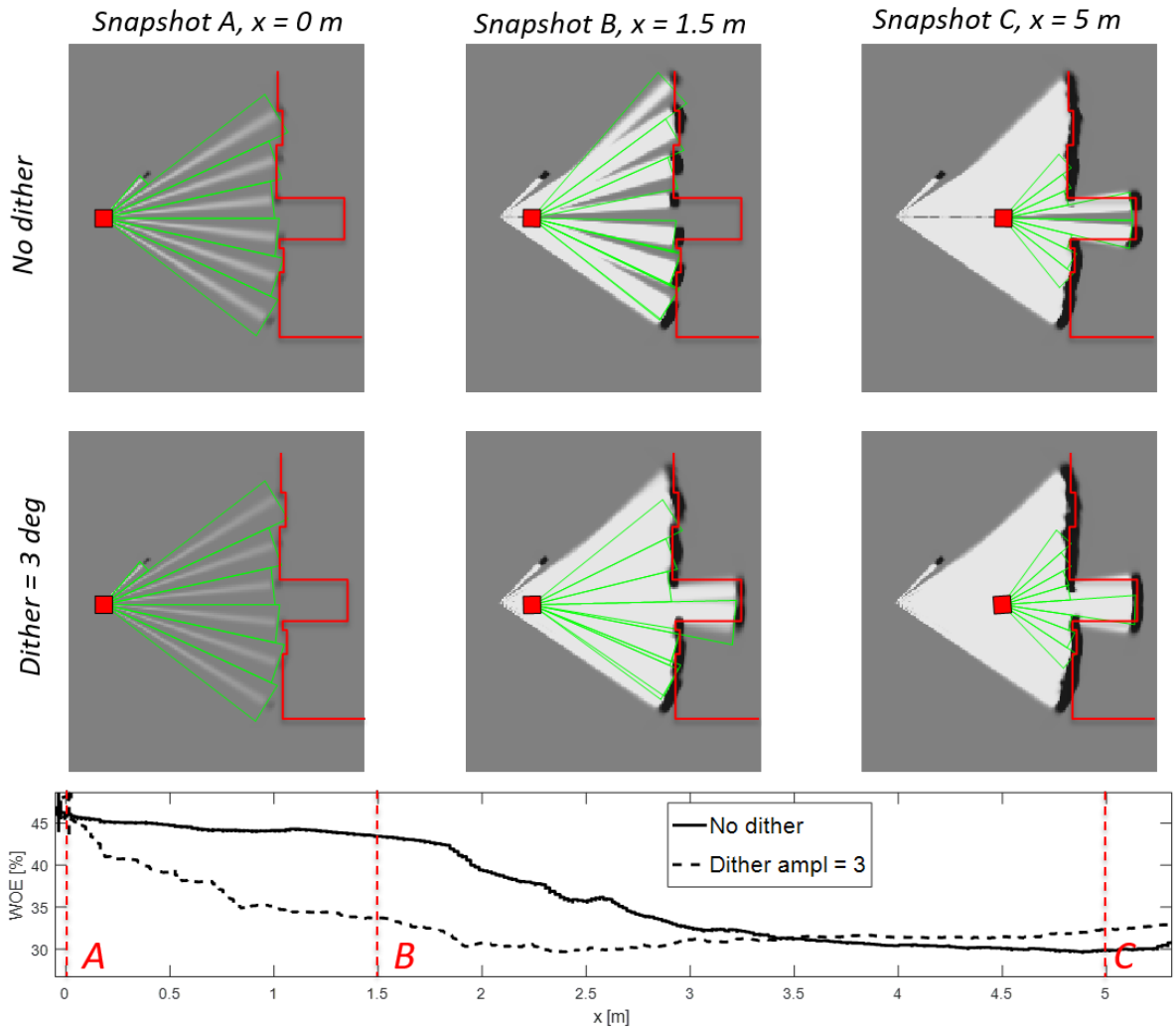

Fig. 9. Incremental mapping

greater area in the environment due to the periodical dither in the robot orientation (see upper-left plot in Figure 7). To have a fair comparison and to be independent from the number of cells evaluated by the LiDAR sensor during a certain trajectory, the concept of spanned region is introduced. This region is defined as the set of cells spanned by the LiDAR diffused light during the robot motion. Also the cells marked occupied in the ground truth map and hit by the laser light are considered in the spanned region. The white area in Figure 8 exemplify the definition of spanned region.

Notice that the cells belonging to the clearance in the wall and at the extreme right of the robot are included in the spanned region even if all the LiDAR measurements corresponds to the closer wall. The spanned region is then incrementally updated: as new cells are evaluated they are added to the spanned region. The WOE is therefore evaluated only for cells belonging to the spanned region: this allows to monitor the map accuracy incrementally and, at the same time, to be independent by the explored area since the metric in Equation (6) is normalized by the total number of cells in the spanned region. The definition of an index that represents the accuracy of the mapping process enables a fine tuning of the *inverse sensor model* described in Section III. Parameters describing the uncertainty in the occupancy grid update such as σ_θ, d_1, d_2 and d_3 were tuned to minimize the WOE while navigating in environments rich of clearance like the one represented in Figure 8.

C. Experiments

A specific experiment has been performed in order to evaluate the robot mapping accuracy while performing a dithering motion. The robot is operated in the environment depicted in Figure 8 and started at 10 meters from the corridor like clearance: the robot is than programmed to follow a straight path towards the clearance. Two versions of the experiment were performed: the first with only the path tracking controller active and no dithering motion, the second with a superimposed dither implemented as explained in Section IV-A. The resulting robot motion derived from the wheel encoders is depicted in Figure 10: the trajectory

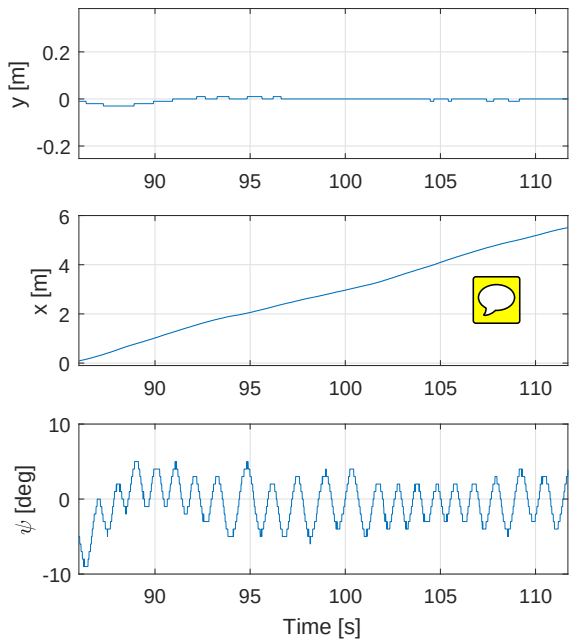

Fig. 10. Robot motion relative to the experiment described in Figure 9. The robot is programmed to follow a straight path with a superimposed dither of around 3 deg amplitude in the robot orientation.

is very close to a straight line but the robot orientation ψ clearly shows the oscillating behavior. Figure 9 shows the mapping results of the two experiments comparing the case with the dithering motion and the one without dithering: three snapshots of the map that is incrementally updated while the robot is moving are depicted together with the WOE describing instant by instant the mapping accuracy as a function of the distance traveled. In both cases the robot starts from the same position and the WOE is around 50% corresponding to the maximum uncertainty level (Snapshot A). After 1.5 meters traveled, it can be noticed that the WOE for the dither case is lower than the one without dither indicating a better mapping accuracy (Snapshot B). This is due to the fact that the dithering motion enabled the detection of the clearance in the wall that is represented fairly well in the map: the oscillating motion infact periodically aligns one of the LiDAR detection segments with the clearance. When this happens the occupancy probability of the free space in the clearance can be correctly updated. As the robot gets closer and closer to the clearance, even without the dithering motion the clearance is detected and represented in the map: this moment is depicted in Snapshot C where the WOE of both cases settles around 30%. Actually in Snapshot C, the accuracy of the non dither case is slightly superior to the dither case: this maybe due to the fact that the estimation of the robot pose performed through the simple wheel encoders integration accumulates a greater error in the case of the dithering motion.

V. CONCLUSIONS

In this paper the possibility of superimposing a small oscillating motion to a given robot path is explored in order to improve the mapping accuracy of the environment. Preliminary experimental results showed that, even a small oscillation that do not visibly modify the given path, can help in speeding up the detection of corridor like clearances. This technique especially suits cases where sensors with long range capabilities but small angular resolutions are employed such as the innovative Solid State LiDAR used in this work. The classical log-odds formulation of the occupancy grid update is used based on the inverse sensor model. Future work will focus, beside a more extensive experimental campaign, on the development of a forward sensor model for the Solid State LiDAR to verify if a forward approach to the occupancy grid problem can further enhance the mapping performance with the dithering technique presented.

REFERENCES

[1] Wurm, Kai M., Cyrill Stachniss, and Giorgio Grisetti. "Bridging the gap between feature-and grid-based SLAM." Robotics and Autonomous Systems 58.2 (2010): 140-148.

[2] Grisetti, Giorgio, Cyrill Stachniss, and Wolfram Burgard. "Improved techniques for grid mapping with rao-blackwellized particle filters." IEEE transactions on Robotics 23.1 (2007): 34-46.

[3] Elfes, Alberto. "Using occupancy grids for mobile robot perception and navigation." Computer 22.6 (1989): 46-57.

[4] Konolige, Kurt. "Improved occupancy grids for map building." Autonomous Robots 4.4 (1997): 351-367.

[5] Lee, Kyoungmin, and Wan Kyun Chung. "Effective maximum likelihood grid map with conflict evaluation filter using sonar sensors." IEEE Transactions on Robotics 25.4 (2009): 887-901.

[6] Thrun, Sebastian. "Learning occupancy grid maps with forward sensor models." Autonomous robots 15.2 (2003): 111-127.

[7] Colleens, Thomas, and J. J. Colleens. "Occupancy grid mapping: An empirical evaluation." Control & Automation, 2007. MED'07. Mediterranean Conference on. IEEE, 2007.

[8] Borenstein, Johann, and Yoram Koren. "The vector field histogram-fast obstacle avoidance for mobile robots." IEEE transactions on robotics and automation 7.3 (1991): 278-288.

[9] Joho, Dominik, et al. "Autonomous exploration for 3D map learning." Autonome Mobile Systeme 2007. Springer, Berlin, Heidelberg, 2007. 22-28.

[10] Stachniss, Cyrill, Giorgio Grisetti, and Wolfram Burgard. "Information Gain-based Exploration Using Rao-Blackwellized Particle Filters." Robotics: Science and Systems. Vol. 2. 2005.

[11] Kaufman, Evan, Taeyoung Lee, and Zhuming Ai. "Autonomous exploration by expected information gain from probabilistic occupancy grid mapping." Simulation, Modeling, and Programming for Autonomous Robots (SIMPAR), IEEE International Conference on. IEEE, 2016.

[12] Thrun, Sebastian, Wolfram Burgard, and Dieter Fox. Probabilistic robotics. MIT press, 2005.

[13] website: www.leddartech.com, 2018

[14] Choset, Howie M. Principles of robot motion: theory, algorithms, and implementation. MIT press, 2005.

[15] de Wit, Carlos Canudas, Bruno Siciliano, and Georges Bastin, eds. Theory of robot control. Springer Science and Business Media, 2012.

[16] Balaguer, Benjamin, et al. "Evaluating maps produced by urban search and rescue robots: lessons learned from RoboCup." Autonomous Robots 27.4 (2009): 449.

[17] Carlson, Jennifer, et al. "Conflict metric as a measure of sensing quality." Robotics and Automation, 2005. ICRA 2005. Proceedings of the 2005 IEEE International Conference on. IEEE, 2005.